ELSEVIER

Journal of Nuclear Materials 313–316 (2003) 909–913

journal of nuclear materials

www.elsevier.com/locate/jnucmat

Improved modelling of detachment and neutral-dominated regimes using the SOLPS B2–Eirene code

X. Bonnin [a,*], D. Coster [b], C.S. Pitcher [c], R. Schneider [a], D. Reiter [d], V. Rozhansky [e], S. Voskoboynikov [e], H. Bürbaumer [f]

[a] *Max-Planck-Institut für Plasmaphysik, Teilinstitut Greifswald, Bereich Stellaratortheorie, EURATOM-Association, Wendelsteinstrasse 1, D-17491 Greifswald, Germany*

[b] *Max-Planck-Institut für Plasmaphysik, EURATOM-Association, D-85748 Garching, Germany*

[c] *Plasma Science and Fusion Center, Massachusetts Institute of Technology, Cambridge MA, 02139, USA*

[d] *Institut für Plasmaphysik, Forschungszentrum Jülich GmbH, EURATOM Association-KFA, Trilateral Euregio Cluster, D–52425 Jülich, Germany*

[e] *St. Petersburg State Technical University, 195251, St. Petersburg, Russia*

[f] *Institut für Allgemeine Physik, TU Wien, Wiedner Hauptstrasse 8–10, A–1040 Vienna, Austria*

Received 27 May 2002; accepted 12 September 2002

Abstract

In this paper, recent progress in plasma edge modelling is presented, using the SOLPS B2–Eirene Scrape-Off Layer Plasma Simulation code. The code capabilities have been extended so that is it now possible to investigate reliably regimes dominated by strong neutral sources in the plasma edge. Two main improvements are reported. First, a fluid plasma treatment including drift and currents effects has been coupled to a Monte-Carlo treatment for the neutrals. Concurrently, a grid adaptation algorithm compatible with the coupling is demonstrated. We present simulations taking advantage of these new tools, and discuss their impact on the results.

PACS: 52.65.−y; 52.65.Kj; 52.65.Pp; 52.55.Fa
Keywords: Edge modelling; Adaptive grids; Drifts; Neutral modelling

1. Introduction

The importance of neutral fluxes in the plasma edge of magnetic fusion devices has long been recognized [1]. Thus, a large amount of effort has been put toward the inclusion of neutrals in plasma edge simulation codes. In the case of fluid codes, one can add a neutral fluid to the equations, but, unless one treats the full 3-D Navier–Stokes system [2], this solution is at best approximate and often inappropriate. A favored approach is therefore to couple the fluid description of the ionized plasma species with a kinetic Monte-Carlo treatment of the neutrals. The B2–Eirene suite of codes is a successful example of this method [3]. In this paper, we wish to report on recent improvements and issues involved in the handling of such a coupled system. In Section 2, we discuss the situation of a plasma whose sources are neutral dominated, i.e. a case undergoing strong volume recombination. In Section 3, we address the interplay between plasma $\mathbf{E} \times \mathbf{B}$ drifts and neutrals. In Section 4, we present a case where recent improvements in the code, designed to allow for dynamic mesh adaptation, are used in conjunction with the Eirene neutral Monte-Carlo model.

* Corresponding author. Tel.: +49-3834 882 416; fax: +49-3834 882 409.
E-mail address: xpb@ipp.mpg.de (X. Bonnin).

0022-3115/03/$ - see front matter
PII: S0022-3115(02)01475-7

2. The case of strong neutral sources

The principle of coupling a plasma fluid code and a Monte-Carlo neutral code is relatively simple: the fluid code computes a plasma background on which neutral particles are followed according to some Monte-Carlo methods; the trajectories of these neutral particles are then integrated to yield information about the sources and sinks due to neutral–plasma interactions (charge-exchange, ionization, recombination, etc...); these sources and sinks are then fed back to the fluid code which computes a new plasma background, and the cycle repeats itself until convergence. Further refinements can include, on the neutral code side, self-consistent neutral–neutral interactions, or radiation transport [4]. On the fluid code end, one must take care that the neutral particle and energy sources or sinks are not too large compared to the plasma particle and energy content.

This is particularly true for volume recombination, for example in detaching plasmas. As the plasma temperature decreases below 1 eV, the recombination rate rises steeply and causes large neutral density increases. In a coupled codes set-up, then, low temperature areas will feel large energy and momentum sinks as the recombined neutrals diffuse away, getting ionized and/or charge-exchanging in the surrounding plasma, cooling it and triggering even more recombination. Physically, this instability is balanced by the fact that, at very low temperatures, three-body recombination actually heats the plasma [5]. However, in order to numerically obtain such stabilization, one is forced to very small timesteps (of the order of 10^{-8} s, essentially running the code in a fully time-dependent fashion), to allow the plasma quantities to re-equilibrate self-consistently. Because such small timesteps are prohibitive, we have chosen, in cases where only the final steady-state is of interest, to rescale the recombination sources in B2–Eirene instead. By rescaling, we mean that, from one timestep to the next, we only allow the sources and sinks associated with any species of recombining neutrals to grow by at most a certain amount (typically 10%). This rescaling slows down the numerical onset of volume recombination, and provides much better code stability. An example is shown in Fig. 1. In this case, the timestep chosen is 10^{-3} s (only a small fraction of the run history is shown). The figure shows the quick onset of massive volume recombination ('no scaling' curve in Fig. 1, going from a few Amperes at iteration 15 to nearly 1000 A ten iterations later), while the source in the fluid code (curve 'with scaling' in Fig. 1) grows much slower. Without such rescaling, the ion energy content of the recombining region would collapse and the run terminate. Yet, the rescaling has no influence on the final steady state reached by the solution (much later than the end of the figure), as the two recombination fluxes eventually come together. The figure also shows that this scaling is carried over when restarting a run from a saved state. On the first iterations, the fluid code continues with the moderate recombination flux inherited from the previous code run, while the kinetic code is going through the end of a recombination event, which is usually as abrupt as its onset.

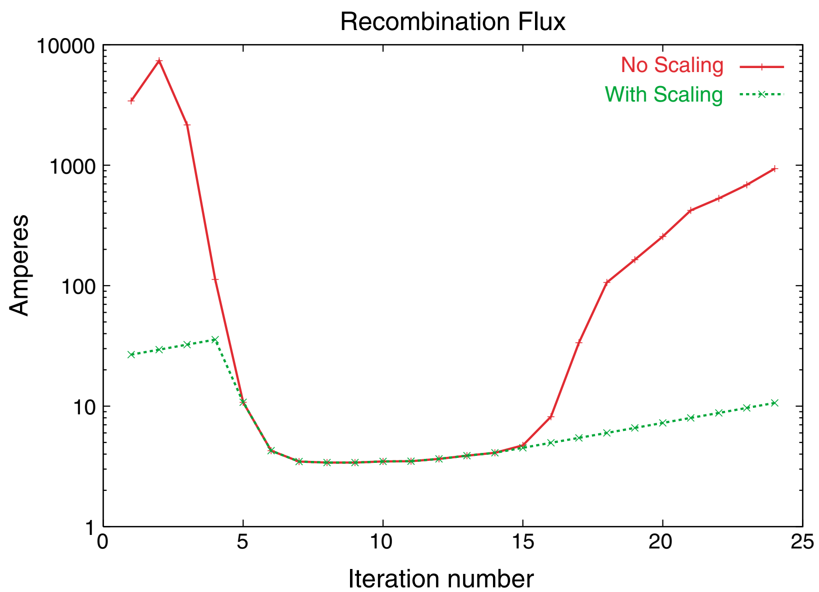

Fig. 1. Scaling of the volume recombination fluxes. The amount of volume recombination given by the Monte-Carlo code (solid line) is scaled to the dashed line in the fluid code.

3. Drifts and currents in the presence of neutrals

In this section, we present results of the first coupled B2–Eirene simulations where drift and currents have been included. Specifically, $\mathbf{E} \times \mathbf{B}$ drifts, and cross-field current terms such as parallel viscosity-driven and ion-neutral friction currents are taken into account [6,7]. No diamagnetic terms are present, for reasons discussed below, although such additional terms are expected to be significant. The case is a standard medium-density Alcator C–Mod discharge. We chose C–Mod because its combination of compact size, high field and high density ensures large field strength gradients, strong drifts and large neutral effects. The relevant boundary conditions for our case are $P_{\mathrm{heat}} = 1.1$ MW and $n_e = 8.0 \times 10^{19}$ m^{-3} at the core boundary, and decay lengths of 0.01 m at the private flux and SOL outer boundaries for n_e, T_e and T_i. We have set $\chi_e = \chi_i = 0.4$ m^2/s, and $D_\perp$ varies from 0.3 m^2/s at the separatrix to 2.5 m^2/s in the far SOL, which gives a good match to typical C–Mod experimental results [9].

We illustrate the impact of the drifts and the neutrals in Fig. 2, with the variation of the poloidal velocity across the outer and inner midplane for several cases: without drifts and 'normal' toroidal field ($\mathbf{B}_t$) direction, that is $\mathbf{B} \times \nabla B$ pointing towards the X-point; with $\mathbf{E} \times \mathbf{B}$ drift and normal $\mathbf{B}_t$ direction; with $\mathbf{E} \times \mathbf{B}$ drift and $\mathbf{B}_t$ inverted; without drifts but with $\mathbf{B}_t$ inverted; and using the code version SOLPS6.0 with grid adaptation, without drifts but the normal $\mathbf{B}_t$ direction (see Section 4 below). The flow pattern remains dominated by the neutral recycling sources and the overall plasma solution (in terms of density and temperature profiles, both at the plates and the midplane) changes relatively little with or without $\mathbf{E} \times \mathbf{B}$ drifts, for both directions of $\mathbf{B}_t$. It is also interesting to note that the plasma flow near the separatrix remains towards the inner divertor, even at the outer midplane, although the location of the poloidal stagnation point is quite dependent on the presence and sign of drifts. Unfortunately, it was not possible to compare with a fluid neutrals case, as such cases tended to strongly recombine and/or crash for the parameters chosen here. Indeed, fluid neutral cases start recombining and detaching for very low core electron densities (a few 10^{19} m^{-3}), while coupled cases remain stable, more in agreement with experiment.

In Fig. 3, we show a set of trajectories of ions produced from ionizing recycled neutrals. The startpoints of these trajectories are created according to the local strength of recycled neutrals ionization. Thus the figure shows the flow pattern felt by newly ionized particles. In all cases, one finds a potential hill centered around the X-point, which height remains roughly constant. In general, most of the recycling takes place at the level of the X-point or below, and there is strong plasma plugging of the divertor: little of the recycled neutral flux

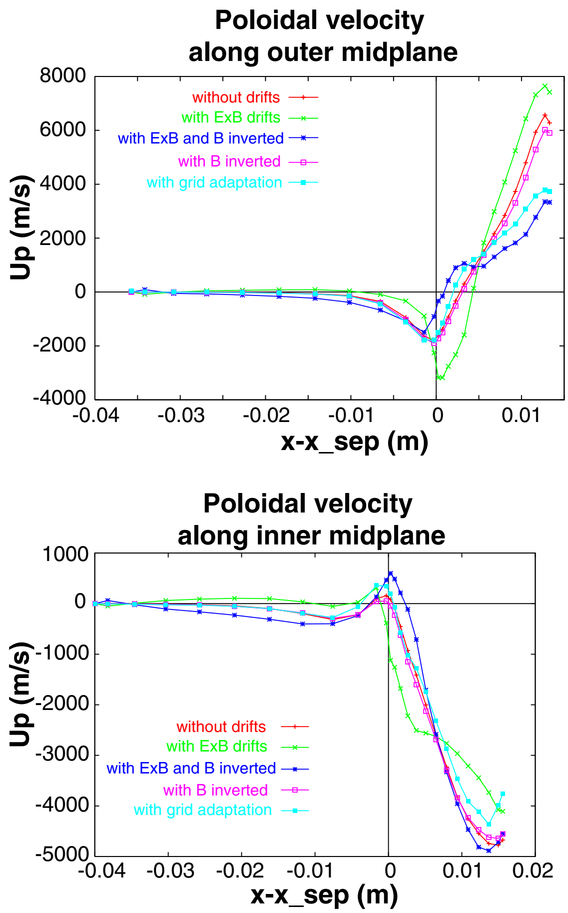

Fig. 2. Radial profiles of the plasma poloidal velocity along the inner (bottom) and outer (top) midplanes for a variety of conditions: without drifts and normal $\mathbf{B}_t$ direction, with $\mathbf{E} \times \mathbf{B}$ drifts and normal $\mathbf{B}_t$ direction, with $\mathbf{E} \times \mathbf{B}$ and B inverted, with $\mathbf{B}$ inverted but no drifts, and using the code version with grid adaptation without drifts and the normal $\mathbf{B}_t$ direction. Positive abscissae indicate the SOL. Negative values of the velocity mean flow directed towards the inner divertor. Note that, close to the separatrix, the flow at the outer midplane is still directed towards the inner divertor.

from the divertor reaches the main plasma. What does reach the main plasma tends to make a (counter) clockwise rotation around the potential hill at the X–point and not penetrate very deeply, for normal (inverted) $\mathbf{B}_t$. The ions produced from main chamber recycling are preferentially flowing towards the inner (outer) divertor, in the presence of $\mathbf{E} \times \mathbf{B}$, for normal (inverted) $\mathbf{B}_t$. In the absence of drifts, there is very little circulation around the X–point and the main chamber recycling is roughly balanced between inner and outer divertors.

Several physics issues remain to be addressed before the drifts and currents model pictured here is fully

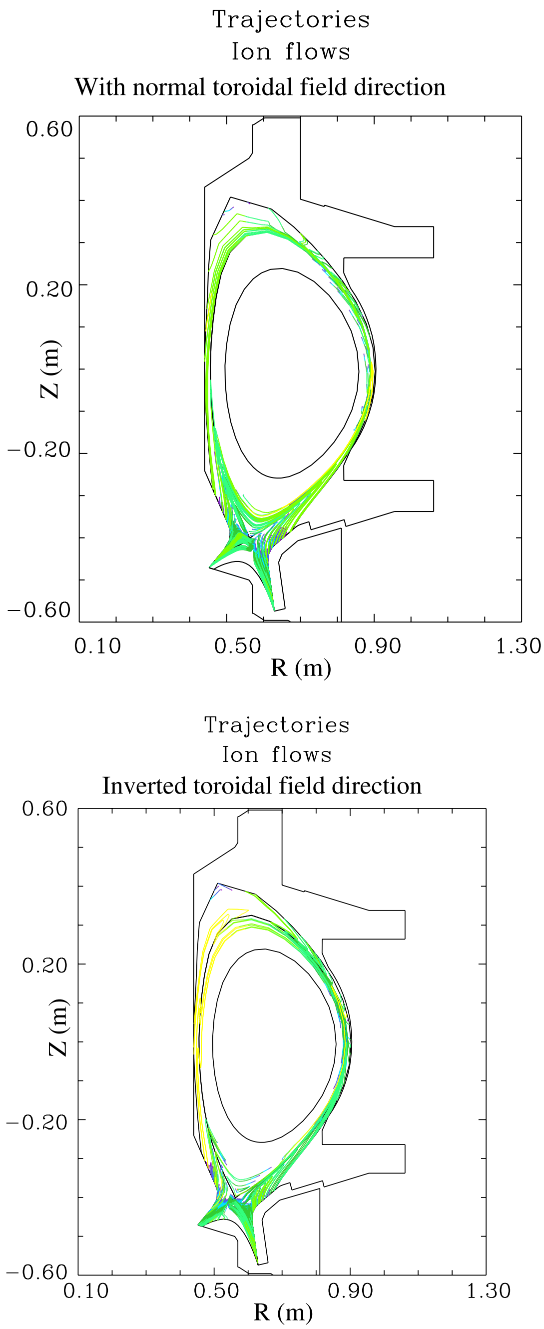

Fig. 3. Ion trajectories, for the coupled case with $\mathbf{E} \times \mathbf{B}$ drifts and $\mathbf{B}_t$ in the ordinary direction (top) or inverted (bottom). The start points of the trajectories are randomly sampled according to the local strength of the ionization of neutrals by the plasma. The color scheme, from purple to green to yellow, refers to the relative length of time a particle takes to follow a given trajectory (purple is shortest, yellow is longest). Three features appear clearly: most of the ionization takes place just under the X-point, neutrals ionized in the main chamber travel preferrentially to the inner (outer) divertor, and a (counter-)clockwise flow loop is formed around the X-point, for normal (inverted) $\mathbf{B}_t$ direction.

self-consistent. The Eirene code must know about the electric potential, solved in B2.5, to properly follow the trajectories of molecular ions (such as D_2^+) including drifts. Similarly, Eirene should compute the perpendicular momentum sinks due to neutrals, in both the radial and diamagnetic directions, which are necessary to compute ion-neutral friction-induced currents. For now, this effect is computed only from a residual fluid neutral population in B2.5, i.e. is vanishingly small. Of more fundamental importance, a distinction must be made between the diamagnetic velocity as understood in a fluid or a kinetic context. In B2.5, only the divergent part of the diamagnetic terms are computed [6]. In a kinetic model, though, it is the total diamagnetic velocity which is needed, to properly describe the local drifting plasma Maxwellian with which the neutrals interact. Moreover, there are, independent of neutral coupling, critical questions about how one should handle the radial boundary condition for the current continuity equation at the plasma core boundary, which are beyond the scope of this paper. It is expected that, with diamagnetic drifts as well as $\mathbf{E} \times \mathbf{B}$ contributions, the plasma solution could change significantly. These issues, as well as further contributions to the cross-field currents [8] and the inclusion of impurities [10], are currently being included in the standard B2.5 package as part of the ongoing code development.

4. Mesh adaptation including neutral Monte-Carlo modelling

The same case as in Section 3 is considered, without drifts, but now treated with the newest version of the code, which allows for dynamic adaptation of the computational mesh, and has been made compatible with Eirene coupling. As described in [11], we use a two-mesh method, where a basis mesh defines a maximum refinement level, and serves as a scaffolding for the coarser mesh on which the computation takes place. For the case presented here, the initial and basis meshes are identical.

When coupling with Eirene, one can in principle use either mesh to calculate the neutral sources. For convenience, we have opted for the basis mesh. Although this choice means more computation in Eirene (treating more grid surfaces), it was also the simplest to code. The other approach would be to inform Eirene of the changing mesh geometry after each of its rearrangements, which would be best done by halving each of the B2.5 coarse cells into triangles, and using this triangular mesh to compute the Monte-Carlo trajectories.

As one can see from the profiles in Fig. 2, the code with mesh adaptation obtains essentially the same results as the normal case without drifts. We thus demonstrate for the first time successful usage of the grid adaptation in concurrent use with the Monte-Carlo coupling within B2–Eirene.

References

[1] D. Reiter, J. Nucl. Mater. 196–198 (1992) 80.
[2] D.A. Knoll, P.R. McHugh, S.I. Krasheninnikov, D.J. Sigmar, Phys. Plasmas 3 (1996) 293.
[3] R. Schneider, H.-S. Bosch, D.P. Coster, J.C. Fuchs, J. Gafert, et al., J. Nucl. Mater. 266–269 (1999) 175.
[4] D. Reiter, S. Wiesen, M. Born, these Proceedings.
[5] P.C. Stangeby, The Plasma Boundary of Magnetic Fusion Devices, IoP, Bristol, UK, 2000, p. 141ff.
[6] R. Schneider, D. Coster, B. Braams, P. Xantopoulos, V. Rozhansky, S. Voskoboynikov, E. Kovaltsova, H. Bürbaumer, Contrib. Plasma Phys 40 (2000) 328.
[7] V. Rozhansky, S. Voskoboynikov, E. Kaveeva, D. Coster, R. Schneider, Nucl. Fusion 41 (2001) 387.
[8] V. Rozhansky, S. Voskoboynikov, E. Kovaltsova, D. Coster, R. Schneider, Contrib. Plasma Phys. 40 (2000) 423.
[9] C.S. Pitcher, X. Bonnin, C.J. Boswell, B. LaBombard, B. Lipschultz, R. Schneider, J.L. Terry, these Proceedings.
[10] V. Rozhansky, E. Kaveeva, S. Voskoboynikov, A.H. Bekheit, D. Coster, X. Bonnin, R. Schneider, these Proceedings.
[11] X. Bonnin, H. Bürbaumer, R. Schneider, D. Coster, F. Aumayr, H.P. Winter, Contrib. Plasma Phys. 42 (2002) 175.